

Nonlinear luminescence and time-resolved diffusion profiles of photoexcited carriers in semiconductors

A. Olsson,^{a)} D. J. Erskine, Z. Y. Xu,^{b)} A. Schremer, and C. L. Tang
Cornell University, Ithaca, New York 14853

(Received 6 May 1982; accepted for publication 28 July 1982)

We describe a new and general optical technique for studying carrier dynamics in semiconductors which is based on the luminescence nonlinearity resulting from the bimolecular recombination of the carriers. The technique has been used to obtain time-resolved diffusion profiles and the hole mobility in photoexcited GaAs.

PACS numbers: 72.40. + w

In this letter, we report a new and general optical technique for the study of carrier dynamics in semiconductors. We have used this technique to obtain time-resolved carrier diffusion profiles in photoexcited GaAs, showing the temporal and spatial evolution of an initial carrier distribution which approximates a delta function in time and space. The technique is based upon a nonlinearity in the luminescence from the sample resulting from a bimolecular recombination of the carriers. The sample is excited by two short pulses (pump and probe). The part of the detected luminescence originating from the recombination of the carriers generated by the probe pulse with those generated by the pump pulse is isolated through an appropriate signal processing scheme. With the additional facility of scanning the pump pulse spot on the sample the spatial distribution of the carriers has been measured with a resolution of better than $2\ \mu\text{m}$.

The existence of a nonlinearity in the generation of the luminescence from the sample is of crucial importance for this type of measurement. Previously, Mahr and Sagan¹ have used another type of nonlinearity (saturation) in the luminescence from an organic dye sample to measure the luminescence lifetime of the dye molecules. Picosecond correlation effects in the hot luminescence of GaAs have been studied by Von der Linde *et al.*, and the relaxation of minority carriers in the picosecond regime in *p*-type GaAs has been measured by Rosen *et al.* using a population-mixing technique.²

The experimental setup is shown in Fig. 1. The light source is a synchronously pumped DCM-dye laser operating at 650 nm with a pulse width of 4 ps. To decrease the average optical power on the sample and to increase the pulse separation, an acousto-optic modulator was used to select one out of every 96 pulses from the dye laser. The 1-MHz optical pulse train is split at a polarizing beam splitter (PBS) in two orthogonal polarized beams of equal intensity. The two beams are later recombined on a second PBS and focused onto the sample with a 4-mm microscope objective (MO). The pump beam is chopped at 200 Hz and passes through an optical system consisting of two lenses (L1 and L2) and a scanning mirror (SM) which allows for the pump spot to be scanned across the sample. With proper adjustment of the lenses L1 and L2 and of the scanning mirror, the input angle of the pump beam to the MO can be continuously varied

while the pump beam entering the MO remain collimated and without translation over the microscope objective lens. With the actual configuration used, the pump spot could be scanned $50\ \mu\text{m}$ on each side of the probe pulse spot. The resolution and linearity of the scanning system were checked by replacing the sample with a reflection grating and recording the backscattered light. The resolution was found to be better than $2\ \mu\text{m}$ over the entire scan range. The luminescence from the sample which is collected by the MO is reflected off a dichroic mirror and focused onto an avalanche photodiode (APD) after passing through a color filter. The signal processing scheme which is outlined in Fig. 1 consists of a sampling scope operating in a boxcar averager mode (BCI) followed by two lockin amplifiers connected in tandem. The effective gate width of the boxcar integrator is 0.5 ns, limited by the time response of the APD. The 0.5-ns time resolution was sufficient for this experiment. However, if higher time resolution is required, the boxcar can be replaced by a up-conversion light gate³ giving a time resolution limited by the duration of the optical pulse, which can be in the subpicosecond regime.^{4,5}

The arrangement of two lockin amplifiers in tandem ensures that only luminescence generated by carriers from the probe pulse which recombine with carriers generated by the pump pulse is detected and displayed on the chart recorder (CR). The final signal at the output from the second

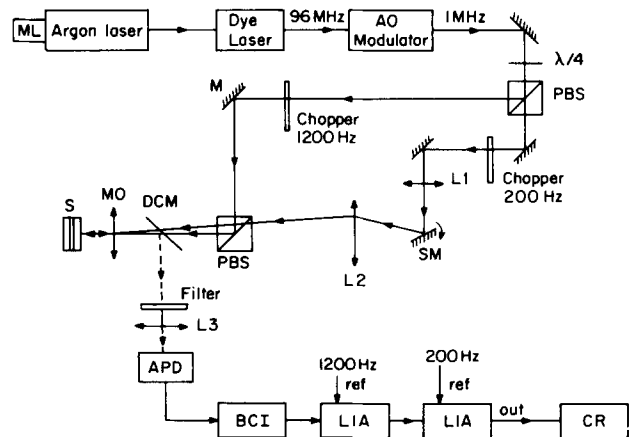


FIG. 1. Experimental setup. ML = mode locker, AO = acousto-optic modulator, PBS = polarizing beam splitter, SM = scanning mirror, L1, L2, L3 = lenses, DCM = dichroic mirror, APD = avalanche photodiode, BCI = boxcar integrator, LIA = lock-in amplifier.

^{a)} Now at Bell Telephone Labs., Murray Hill, New Jersey.

^{b)} On leave from Institute of Semiconductors, Chinese Academy of Sciences, Beijing, P.R.C.

LIA will in fact be proportional to the amount of overlap between the carrier distributions generated by the pump and probe pulse. When the pump and probe beams have equal intensity and strike the sample simultaneously, a spatial autocorrelation of the charge distribution is obtained when the pump spot is scanned across the probe spot. By varying the delay between the sample excitation and the luminescence sampling, the time evolution of the charge distribution is obtained.

The sample studied is a

$\text{Ga}_{0.5}\text{Al}_{0.5}\text{As-GaAs-Ga}_{0.5}\text{Al}_{0.5}\text{As}$ double heterostructure grown by liquid phase epitaxy (LPE). The two GaAlAs cap layers serve several purposes. First they effectively confine the photogenerated carriers to the $1.3\text{-}\mu\text{m}$ -thick GaAs layer (the cap layers are transparent to the excitation light). Second, the cap layers will reduce the surface recombination velocity at the GaAlAs-GaAs interface to approximately 300 cm/s whereas a free-GaAs surface would have a recombination velocity of $5 \times 10^5\text{ cm/s}$.⁶ Third, since the diffusion length L_n is much longer than the GaAs layer thickness the diffusion is two dimensional which simplified the analysis and interpretation of the data.

For the excitation densities used in these experiments ($\sim 7 \times 10^{18}\text{ cm}^{-3}$) and the background doping density of this sample ($\sim 2 \times 10^{15}\text{ cm}^{-3}$) the carrier recombination will be dominated by the bimolecular recombination. This is illustrated in Fig. 2 which shows the luminescence decay for a fixed input pulse energy of $1.5 \times 10^{-10}\text{ J}$ but for different spot sizes on the sample. The curves A-F in the insert of Fig. 2 show the recorded decays for spot sizes ranging from 7×10^{-8} to $3 \times 10^{-4}\text{ cm}^2$. As expected the decay rates are strongly density dependent and the initial decay rate varies over several orders of magnitude. The decays for the highest excitation densities are nonexponential. However, in the low excitation limit, the decays become exponential with a limiting time constant of 350 ns , which probably originates from the residual surface recombination at the GaAs-GaAlAs interface.

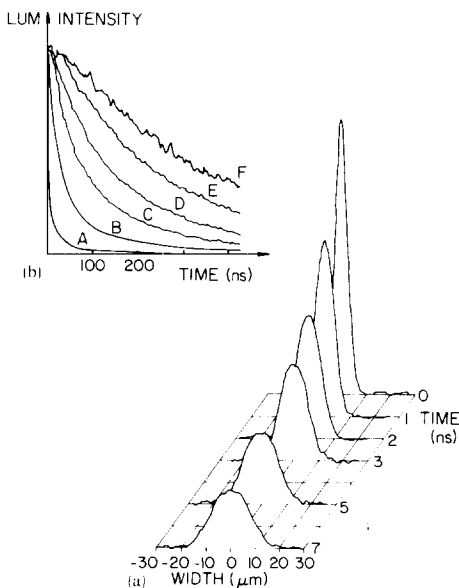


FIG. 2. (a) Recorded time evolution of the autocorrelation of the charge distribution. (b) Luminescence decay curves for a fixed input pulse energy of $1.5 \times 10^{-10}\text{ J}$ but for a spot size varying from A 7×10^{-8} to F $3 \times 10^{-4}\text{ cm}^2$.

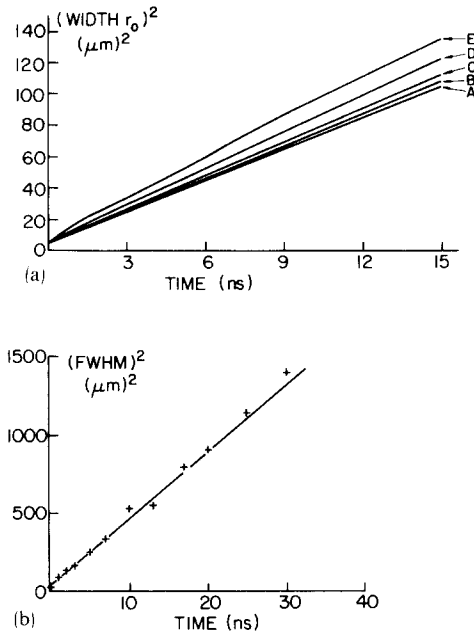


FIG. 3. (a) Charge distribution $(\text{width } r_0)^2$ vs time calculated from the bimolecular diffusion equation. The calculation was done for a nonradiative time constant of 350 ns and a diffusion constant of $17\text{ cm}^2/\text{s}$. Curve A shows the constant lifetime result with a slope of $4D$, and curves B-E are the results for initial densities of 1×10^{18} , 3×10^{18} , 1×10^{19} , and $3 \times 10^{19}\text{ cm}^{-3}$. (b) Measured charge distribution autocorrelation $(\text{FWHM})^2$ vs time.

We will in a separate publication further investigate the luminescence decay from highly photoexcited double heterostructures to complement our previous work on electrically pumped double heterostructure lasers.⁷

A series of recordings of the charge distribution width was made at different delay times from the excitation of the sample. The result is shown in Fig. 2(b), which shows the time evolution of the initial carrier distribution. The initial autocorrelation full width at half-maximum (FWHM) of the charge distribution was $5.3\text{ }\mu\text{m}$ and was limited both by the finite spot size and by the carrier diffusion during the aperture time of the boxcar integrator. In Fig. 3(b) we show the measured $(\text{FWHM})^2$ of the autocorrelation of the charge distribution versus time. The relationship is linear with a slope of $430\text{ cm}^2/\text{s}$. In the following we will show that this is in good agreement with theory and with known material parameters for GaAs.

The bimolecular nature of the carrier recombination in the sample has several implications. One is a nonlinear dependence of the luminescence power on the incident light intensity. For a steady state photoexcited sample, the luminescence power can be obtained from the results given in Ref. 7:

$$P_{\text{lum}} = C \left[(4P_{\text{in}} T_{\text{nr}}^2 B_r / V h \nu + 1)^{1/2} - 1 \right]^2, \quad (1)$$

where B_r is the recombination coefficient, P_{in} is the incident power, T_{nr} is the nonradiative density-independent lifetime, V is the excitation volume, $h\nu$ is the photon energy, and C is a proportionality constant. We have assumed in Eq. (1) that the carrier density is much larger than the background doping density. From Eq. (1) it follows that the luminescence will follow approximately a power law of the incident power. The exponent varies from 2 at low input powers to 1 at high

input powers. We have observed this behavior in all the samples studied. In the case of large background doping densities, Eq. (1) can be appropriately modified.⁷

The two-dimensional diffusion equation for the photoexcited carriers neglecting bimolecular recombination is

$$D \frac{1}{r} \frac{\partial}{\partial r} r \frac{\partial N}{\partial r} - \frac{N}{T} = \frac{\partial N}{\partial t}, \quad (2)$$

where we have assumed circular symmetry. r is the radius vector, N is the carrier density, D is the diffusion constant, and T is the carrier lifetime. Equation (2) can be solved analytically and the Green's function is

$$N(r, t) = \frac{\sigma_0^2 N_0}{4Dt + \sigma_0^2} \exp\left(\frac{-t}{T}\right) \exp\left(\frac{-r^2}{4Dt + \sigma_0^2}\right), \quad (3)$$

where we have included the finite width σ_0 of the distribution at $t = 0$. Equation (3) shows that the carrier distribution is gaussian and that the (width)² increases linearly in time with a slope of $4D$.

Equations (2) and (3) assume that the carriers have a constant lifetime. To correspond to the experimental conditions, the bimolecular recombination term, $-B_r N^2$, must be added to the LHS of Eq. (2). With the bimolecular term, Eq. (2) cannot be solved analytically simply. However, we have solved it numerically and the results show that the density profiles remain very nearly gaussian and the distribution (width)² increases nearly linearly in time. The slope, which in the constant lifetime model is $4D$, now depends on the initial carrier density. In Fig. 3(a) we show the calculated result for the spreading of the charge distribution. The calculation was done for an initial distribution (width)² of $5 \mu\text{m}^2$ and initial densities ranging from 1×10^{18} to $3 \times 10^{19} \text{cm}^{-3}$. For the bimolecular recombination constant we used $B_r = 1 \times 10^{-10} \text{cm}^3/\text{s}$. As seen from Fig. 3(a) the slope is only weakly dependent on the initial carrier density. For carrier densities less than $1 \times 10^{18} \text{cm}^{-3}$, the slope approaches the value $4D$ corresponding to the constant lifetime case, and at an initial density of $3 \times 10^{19} \text{cm}^{-3}$ the slope is approximately $5D$. To calculate the relationship between the width of the measured autocorrelation scan curves in Fig. 2 and the corresponding charge distribution widths, we will proceed assuming a gaussian charge distribution which, according to the numerical solution of the bimolecular diffusion equation, is a valid approximation.

The signal record with the experimental setup shown in Fig. 1 is proportional to the spatial overlap of the two carrier distributions generated by the pump and probe beams. If N_{probe} and N_{pump} are the carrier densities generated by the probe and pump beam respectively, the signal S is given by

$$S(t) \sim \int N_{\text{pulse}}(\mathbf{r}, t) N_{\text{probe}}(\mathbf{r}, t) dV. \quad (4)$$

For a N_{pulse} and N_{probe} with a gaussian distribution, both with a width of r_0 but separated a distance x_0 , Eq. (4) can be evaluated and the result is

$$S(r_0, x_0) \sim \exp(-x_0^2/(2r_0^2)). \quad (5)$$

From the numerical solution of the bimolecular diffusion equation, r_0 can be put in the following form:

$$r_0^2 = \sigma_0^2 + ADt, \quad (6)$$

where σ_0^2 is the initial width of the carrier distribution and A is a constant between 4 and 5. Hence the (FWHM)² of the recorded scan curves is given by

$$(\text{FWHM})^2 = 8 \ln 2 (\sigma_0^2 + ADt). \quad (7)$$

Comparing Eq. (7) with the data from Fig. 3(b) gives a diffusion constant of $D = 17 \text{cm}^2/\text{s}$ for the sample. We used a value for A of 4.5 which corresponds to the initial density of $7 \times 10^{18} \text{cm}^{-3}$. Since the sample is lightly doped and highly excited, $n = p$ and the ambipolar diffusion constant is given by⁸

$$D = 2D_c D_h / (D_c + D_h). \quad (8)$$

The electron Hall mobility measured on a sample from the same growth run was $7000 \text{cm}^2/\text{Vs}$. Using the Einstein relation and the measured ambipolar diffusion constant of $17 \text{cm}^2/\text{s}$ we obtain a hole drift mobility of $340 \text{cm}^2/\text{Vs}$, which compares reasonably with accepted values in the literature.

In conclusion, we have described a new experimental technique with wide applicability in the study of carrier dynamics in semiconductors. The method is based upon the non-linearity in the luminescence which results from the bimolecular recombination of the carriers. In one application of this method, we have obtained time-resolved carrier profiles of a diffusing carrier distribution. This can be a useful non-destructive technique for measuring on a microscopic scale the uniformity of the transport parameters of materials prior to device processing. Other immediate applications include for example measurements of drift velocity and charge packet broadening under external fields.⁹

We thank Professor C. A. Lee for helpful discussions and P. Goodwin for assistance with the computer graphics. This work was supported by the National Science Foundation through the Materials Science Center of Cornell University, Ithaca, NY 14853, and in part by the Joint Services Electronics Program.

¹H. Mahr and A. G. Sagan, *Opt. Commun.* **39**, 269 (1981); H. Mahr, A. G. Sagan, C. P. Hemmenway, and N. J. Frigo, *Chem. Phys. Lett.* **79**, 503 (1981).

²D. von der Linde, J. Kuhl, and E. Rosengart, *J. Lumin.* **24/25**, 675 (1981); D. Rosen, A. Doukas, Y. Budansky, A. Katz, and R. R. Alfano, *Appl. Phys. Lett.* **39**, 671 (1981).

³M. A. Dugay and J. W. Hansen, *Appl. Phys. Lett.* **13**, 178 (1968).

⁴J.-M. Halbout, A. Olsson, and C. L. Tang, *Appl. Phys. Lett.* **39**, 463 (1981); J. Halbout and C. L. Tang, *Appl. Phys. Lett.* **40**, 765 (1982).

⁵R. L. Fork, B. I. Green, and C. V. Shank, *Appl. Phys. Lett.* **38**, 671 (1981).

⁶R. J. Nelson and R. G. Sobers, *Appl. Phys. Lett.* **32**, 761 (1978).

⁷A. Olsson and C. L. Tang, *IEEE J. Quantum Electron.* **QE-18**, 971 (1982).

⁸R. A. Smith, *Semiconductors* (Cambridge University, New York, 1978).

⁹J. A. Cooper and D. F. Nelson, *IEEE Electron. Device Lett.* **EDL-2**, 171 (1981); K. K. Thornber, D. F. Nelson, and J. A. Cooper, *Appl. Phys. Lett.* **39**, 843 (1981).